THE AMERICAN SOCIETY OF MECHANICAL ENGINEERS
345 E. 47th St., New York, N.Y. 10017

97-GT-259

A STUDY OF ACOUSTIC RESONANCE IN A LOW-SPEED MULTISTAGE COMPRESSOR

T. R. Camp
Rolls-Royce plc
Derby, U.K.

ABSTRACT

Measurements are presented of a resonant acoustic phenomenon occurring in a low-speed multi-stage compressor. The results show that this phenomenon shares many characteristics with acoustic resonance as measured in high-speed compressors. These similarities include a rotating pressure field, several acoustics frequencies corresponding to different circumferential modes, step changes in frequency as the flow rate is increased, and acoustic frequencies which are independent of flow coefficient, shaft speed and the axial length of the compression system. The paper includes measurements of the helical structure of the rotating pressure field and of the variation in amplitude of the acoustic signal over a stator exit plane.

NOMENCLATURE

a,b	signal amplitude	T	function of time
c	speed of sound in free space	U	blade velocity
Ch	blade chord	v	flow velocity
D	characteristic dimension	v_a	axial flow velocity
f	frequency (Hz)	x	axial distance
k	wavenumber	X	function of axial distance
m	circumferential order		
M	Mach number	ϕ	phase angle
p	static pressure	λ	wavelength
r	radius	θ	circumferential angle
St	Strouhal number	Θ	function of θ
t	time	ω	frequency (rad/s)

INTRODUCTION

An important consideration during the design and development of axial flow compressors is that the amplitudes of blade stresses must remain below critical values at all operating points to ensure adequate fatigue life. Blade vibrations can be excited by a number of mechanisms, of which the most documented phenomena include blade row interaction effects (resulting from the wakes and potential fields of adjacent blade rows), flutter, rotating stall and surge. In recent years another source of blade excitation has been observed which is characterised by:

- frequencies of excitation which are not necessarily integer multiples of the shaft frequency,
- frequencies which change in a way which is not closely related to blade stiffness,
- step changes in the excitation frequency as the compressor shaft speed is changed,
- large amplitude pressure fluctuations which lead to high blade stresses when the pressure fluctuation frequency is coincident with a natural frequency of blade vibration,
- high amplitudes of fluctuating pressure and blade stresses occurring in regions of irregularities in the flow-field such as bleed slots or blade rows operating at extreme incidence.

Although at present the phenomenon is poorly understood, the limited amount of experimental data available suggests that this excitation is associated with a resonant acoustic condition of the compressor annulus and/or bleed cavities. The link with the acoustics of the system has been revealed by measurements of a fluctuating pressure field which rotates about the compressor axis at a speed near to the local speed of sound. Results also show that the phenomenon is sensitive to the annulus geometry and to the compressor inlet conditions in a manner which is consistent with an acoustic signal. Although in the past this phenomenon has been confused with other failure mechanisms such as flutter, sufficient evidence now exists to regard this as a distinct source of blade vibration, which has been termed ‘acoustic resonance’.

The details of this phenomenon are not well understood, partly because there exists only a very limited amount of test data. Measurements of acoustic resonance in high-speed machines have been difficult to obtain for three reasons. Firstly, experimental studies of acoustic resonance on high-speed compressors are difficult to perform because the high blade stresses normally lead rapidly to blade

Presented at the International Gas Turbine & Aeroengine Congress & Exhibition
Orlando, Florida — June 2–June 5, 1997

failure. Secondly, when the phenomenon has been detected in a high-speed compressor, the demands of commercial time scales have meant that once the source of vibration has been removed, by whatever means, compressor development has continued without a thorough investigation of the phenomenon. Thirdly, the financial cost of running a high-speed compressor for sufficient time to complete a full investigation of the phenomenon is very high. In contrast, low-speed compressor rigs offer much lower running costs and are subject to stresses which are several orders of magnitude below their high-speed equivalents. For these reasons, a study of acoustic resonance on a low-speed multistage compressor is very desirable, provided that it can be shown that the low-speed and high-speed phenomena are similar. In the past, measurements of an acoustic resonance on a low-speed compressor have been limited to a single stage machine (first reported by Parker, 1967).

The C106 compressor at the Whittle Laboratory, Cambridge University, is a four-stage low-speed compressor, containing blading which is representative of modern high-speed compressors. The compressor includes a variable stator mechanism which allows the inlet guide vanes and stator blade rows to be easily restaggered. The compressor has a constant outer radius of 254mm and a hub-tip ratio of 0.75. A more detailed description of the compressor is given by Camp (1995). By operating the C106 compressor at high flow coefficients, with the variable stators at certain off-design settings, it was found that the compressor emitted tones at a series of discrete frequencies which could be clearly heard above the blade passing frequency and the background broad-band noise. Because the C106 is a multistage compressor with a flow-field which is representative of contemporary high-speed compressors, this rig is very suitable for a study of acoustic resonance relevant to high-speed machines.

REVIEW OF PREVIOUS WORK

Acoustic resonance has been detected in the past in high-speed and low-speed, single stage and multistage machines but there is little consistency in the understanding of the phenomenon between different classes of machine. This is particularly true of the distinction between low-speed compressors, on which most previous research work has concentrated, and high-speed machines, for which very few detailed measurements of acoustic resonance exist. In this section a brief introduction is given to the structure of acoustic waves in annular ducts. Following this, we consider vortex shedding from struts or blade rows in the compressor as a possible mechanism for exciting a resonant condition.

The Structure of Acoustic Waves in Annular Ducts

The structure of acoustic signals in annular ducts can be calculated by solving the homogeneous wave equation in cylindrical co-ordinates, as outlined in a pioneering paper by Tyler and Sofrin (1962). In a stationary fluid the three-dimensional wave equation simplifies to,

$$\frac{\partial^2 p}{\partial t^2} - c^2 \nabla^2 p = 0 \qquad (1)$$

If we assume a narrow duct and therefore neglect variations in the radial direction, we can assume a solution of the form $p(\theta,t,x) = \Theta(\theta)\,T(t)\,X(x)$. If we consider one component of the time-dependent function T at frequency ω and one component of the circumferentially varying function Θ with order m, amplitude a_m and phase ϕ_m then the functions Θ and T can be combined and, for $x=0$, the solution written as,

$$p(\theta,t,0) = a_m \exp i(m\theta - \omega t + \phi_m)$$

where the real part is implied. Note that it is necessary for m to be an integer so that the variation of pressure in the θ-direction is continuous and repeats every 2π radians, as required by the cylindrical geometry. In this form the pressure distribution at any axial plane can be interpreted as an m-lobed pattern, as illustrated in Figure 1. This pressure distribution rotates at ω/m rad/s and generates at every point a fluctuating pressure at frequency ω. The pattern sweeps the annulus walls at a velocity $r_o\omega/m$ where r_o is the radius of the duct. This velocity can be expressed as a Mach number by dividing by the velocity of sound in free space c,

$$M_\theta = \frac{r_o\omega}{mc} \qquad (2)$$

By subsituting the expression,

$$p(\theta,t,x) = a_m \exp i(m\theta - \omega t + \phi_m) \times X \qquad (3)$$

into equation 1, an ordinary differential equation is obtained for the function X. This can be solved to find,

$$X = b_m \exp(\pm i k_x x) \qquad (4)$$

where b_m is a constant and k_x is the axial wavenumber defined by,

$$k_x = \frac{m}{r_o}\sqrt{M_\theta^2 - 1} \qquad (5)$$

The axial variation in the pressure distribution takes one of two very different forms, depending on the magnitude of the circumferential Mach number M_θ. If M_θ is less than unity, k_x is imaginary and the function X is real. In this case the pressure field decays exponentially in the axial direction with no change of phase. There is no energy transfer in the axial direction and the acoustic wave is described as 'cut-off'. Because energy cannot propagate through cut-off regions, energy which is input to the system by any source of excitation accumulates, and is manifested by high amplitudes of the fluctuating pressure field. If M_θ is greater than unity, k_x is real and the function X is complex. This case corresponds to a pressure wave which propagates in the axial direction with changing phase and no reduction in amplitude. The structure of this wave, which allows energy to propagate in the axial direction, is described as 'cut-on'. The wavefronts of this wave trace out m helices, which rotate about the axis of the duct at ω/m rad/s.

The solution method outlined above assumes a narrow, empty duct at constant radius with no flow. In a real compressor, however, the annulus has a finite span and encloses rotating and stationary blade rows, while the mean flow velocity is normally a significant proportion of the local speed of sound. The annulus areas of real compressors vary in the axial direction, and the temperature of the fluid (and therefore the speed of sound) increases with axial distance. Each of these factors adds considerable complication to the solution of the

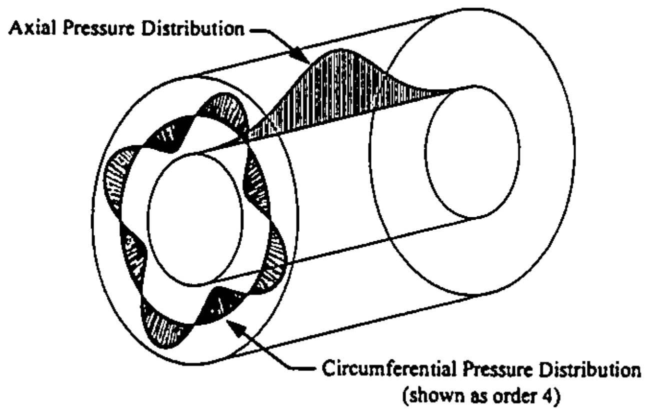

Figure 1. Illustration of circumferential and axial pressure distributions

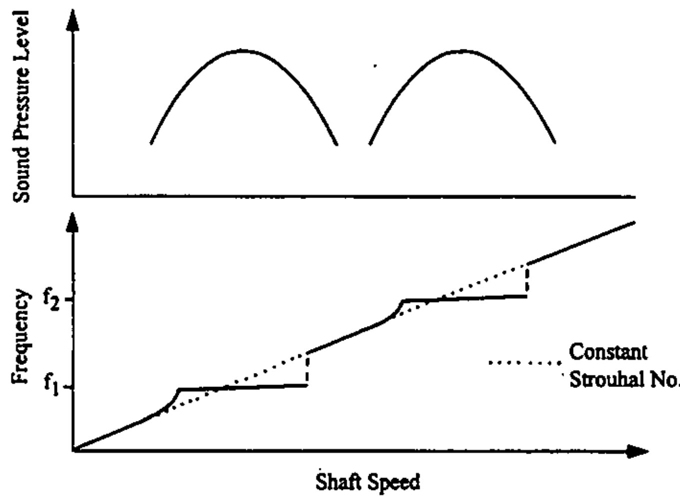

Figure 2. Two 'locked-on' resonant frequencies (after Parker and Stoneman, 1989).

wave equation which, as a result, cannot generally be solved without approximation. Despite these effects, the structure of the wave in the circumferential and axial directions, whether cut-on or cut-off, remains similar to the expressions given above.

Vortex Shedding as an Excitation Mechanism

Having described the structures with which acoustic waves may resonate and propagate in annular ducts, we note that significant amplitudes will only result when there is a source of excitation which provides an energy input to the disturbance. Extensive work by Parker and his colleagues at the University College of Swansea has shown that a possible source of excitation is the mechanism of vortex shedding from struts or blade rows at high incidence (Parker and Stoneman, 1989). The phenomenon of wake excitation of resonances is well known in other areas of engineering; bridges and chimneys, for example, can be forced to resonate by the shedding of vortices. In a similar way, bluff bodies in ducts can shed vortices in their wakes which interact with the flow-field. In the cases of bridges and chimneys, the surrounding fluid is effectively infinite in extent and resonance occurs when the frequency of vortex shedding is equal to, or close to, the natural frequency of mechanical vibration of the structure. In a duct the condition for resonance is subtly different: in this case, acoustic resonance occurs when the natural frequency of vortex shedding is approximately equal to the acoustic resonant frequency of the duct. It has been found that when the natural frequency of vortex shedding is close to the resonant frequency of the duct, the frequency of vortex shedding will 'lock on' to the acoustic frequency (Cumpsty and Whitehead, 1971). If this frequency is also equal to one of the natural frequencies of blade vibration, then the amplitude of the acoustic signal is reinforced and the vibration of the blade can lead to very high mechanical stresses. Blade stresses are found to be particularly large if the vibrating blade is also the source of the shed vortices because the correlation between the vortex shedding and the mechanical vibration is then very high.

For significant blade vibration to occur as a result of a vortex-driven acoustic resonance, there are therefore three frequencies that must approximately coincide: a natural frequency of vortex shedding, an acoustic resonant frequency of the duct (including blades) and a natural frequency of blade vibration. The occurrence of such a event is not as rare as it might first appear when one considers the number of blade rows in a typical compressor, each of which can shed vortices at a number of frequencies (Welsh and Gibson, 1979) and vibrate in several flexural and torsional modes. Acoustic resonance of the duct may also occur at several frequencies corresponding to different circumferential and radial orders.

The frequency at which vortices are shed by a body can be related to its dimensions and the velocity of the fluid by an approximately constant value of the Strouhal number, defined by,

$$\text{Strouhal number} = \frac{f\,D}{v} \tag{6}$$

Previous measurements have shown that the natural frequency of vortex shedding for an isolated flat plate or strut is given by a Strouhal number of approximately 0.20, based on trailing edge thickness. At a resonant condition, however, this value of Strouhal number may change significantly, as shown by Koch, 1985. If the boundary layer thickness at the trailing edge of the body is significant, or if the plate or aerofoil is stalled, the distance between the shear layers on either side of the wake is a more appropriate dimension for the Strouhal number calculation.

For vortex shedding at a constant Strouhal number, the frequency of vortex shedding f is proportional to the velocity v. For a compressor blade row operating at a constant value of flow coefficient, v_a/U, the frequency of vortex shedding is proportional to U and therefore to the shaft speed. As the shaft speed of the compressor increases or decreases, the frequency of vortex shedding will sweep a range of frequencies and will tend to excite the acoustic modes in that range. As the frequency of vortex shedding 'locks on' to different acoustic modes, step changes occur in the frequency of the acoustic signal as illustrated in Figure 2. This stepping in mode or wavenumber is observed in high-speed compressors as one of the distinctive characteristics of acoustic resonance. This observation therefore supports the hypothesis that vortex shedding is the

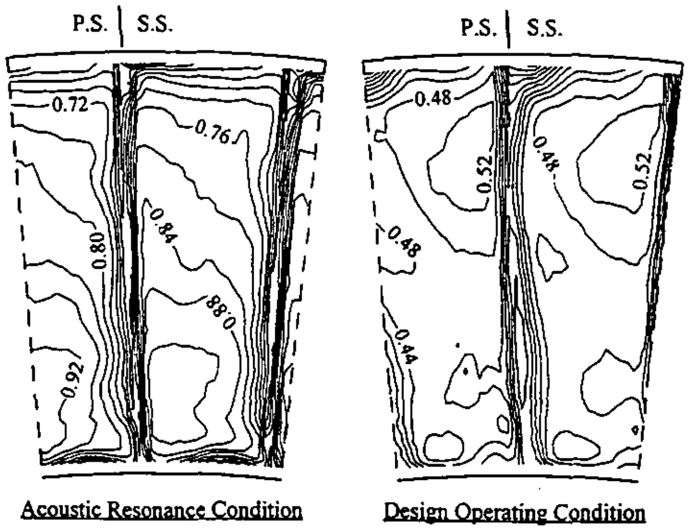

Figure 3. Contours of axial velocity at the stator 3 exit plane (non-dimensionalised by mid-height rotor speed)

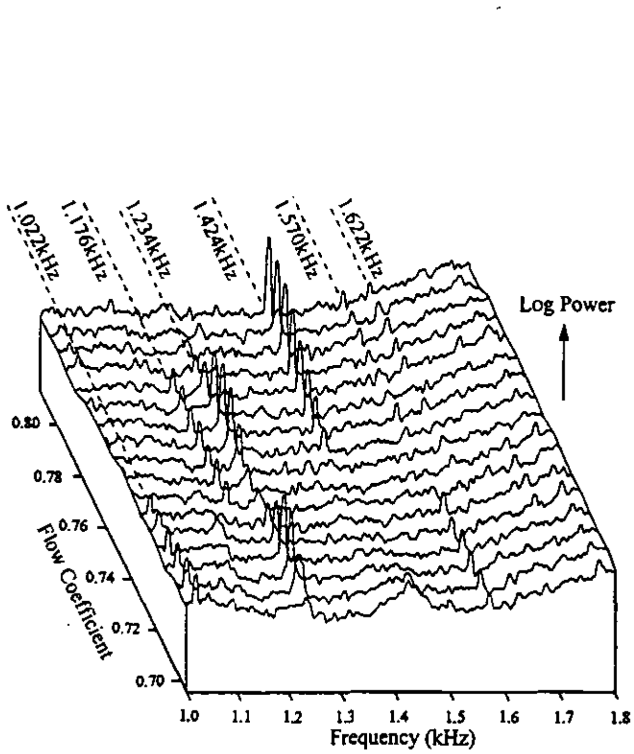

Figure 4. Pressure amplitude spectra as a function of flow coefficient

mechanism by which the resonance is excited. However, at the present time this has only been confirmed experimentally at low Mach numbers in cascades and in a single-stage low-speed compressor.

EXPERIMENTAL RESULTS FROM A LOW-SPEED COMPRESSOR

Rig Geometry and Instrumentation

An acoustic phenomenon was first detected on the C106 compressor at a high flow operating point when the stagger angles of the IGV and stator blade rows were reduced by 10° from their design settings. Because the main purpose of these experiments was to assess the similarity of the phenomenon to acoustic resonance as found in high-speed machines, no attempt was made to map the phenomenon over a range of stagger angles or flow coefficient. Instead, a geometry and flow coefficient were chosen at which the amplitude of one of the acoustic signals (at 1420Hz) was significantly larger than signals at surrounding frequencies, thereby making this signal easier to measure. Accordingly, all experiments were performed with the stagger of the IGV and all stator rows reduced by 10° from their design values and, unless otherwise stated, at a flow coefficient of 0.85.

At this operating point the rotor incidence angle was -9.6° at mid-span while the stator incidence was approximately -25°. Previous experience from high-speed compressors suggests that when acoustic resonance is associated with a mis-matched blade row, it is normally associated with high positive incidence. However, negative incidence angles can cause similarly wide wakes and could therefore cause vortices to be shed at similar frequencies. The axial velocity field was measured downstream of the stator 3 exit plane at the test operating point. In Figure 3 the measured flowfield is compared with the flowfield at the design operating condition, showing the increased width of the stator wake on the pressure side of the blade at the acoustic resonance condition.

For most of the experiments described in this paper, the acoustic signal was measured using arrays of Kulite transducers. These transducers were mounted flush with the outer annulus wall of the compressor, a position which gave two advantages: firstly the annulus walls are always pressure antinodes regardless of the radial order of the signal (the radial pressure gradient must be zero at a hard wall) and so the pressure signal was always clear, and secondly, in this position the transducers offered no obstruction to the flow. It was found that high frequency-response pressure transducers were more sensitive to the acoustic signal than hot-wire probes.

Preliminary Spectral Analysis

After first detecting the acoustic signals as audible tones above the background noise of the compressor, a preliminary investigation was made using a pressure transducer and a spectrum analyser. The transducer was used to measure static pressure perturbations at the compressor inlet plane over a range of flow coefficient between 0.70 and 0.81. Figure 4 shows the measured spectra for frequency components between 1.0 and 1.8kHz. The spectra in Figure 4 show clear peaks at six frequencies, of which the most prominent and most audible signal was at 1.424kHz. Although this figure suggests that each peak covers a considerable range of frequencies, this is a consequence of the short sampling period used by the spectrum analyser. Measurements made using a longer sampling period showed that each acoustic signal occupied a very narrow bandwidth. Of the six peaks identified in Figure 4, four of these occur at frequencies which are close to integer multiples of 204Hz, as shown in Table 1. This relationship was first identified by Cargill (1993).

Table 1 suggests that the four signals are consistent with rotating pressure patterns of orders 5, 6, 7 and 8. (The observation that the relationship between frequency and mode number is not *exactly* linear is consistent with previous measurements, such as those reported by Parker, 1968). Assuming that this is the case, a Mach number based on the circumferential phase velocity at the tip radius and the speed of sound in free space can be calculated approximately using equation 2 as follows,

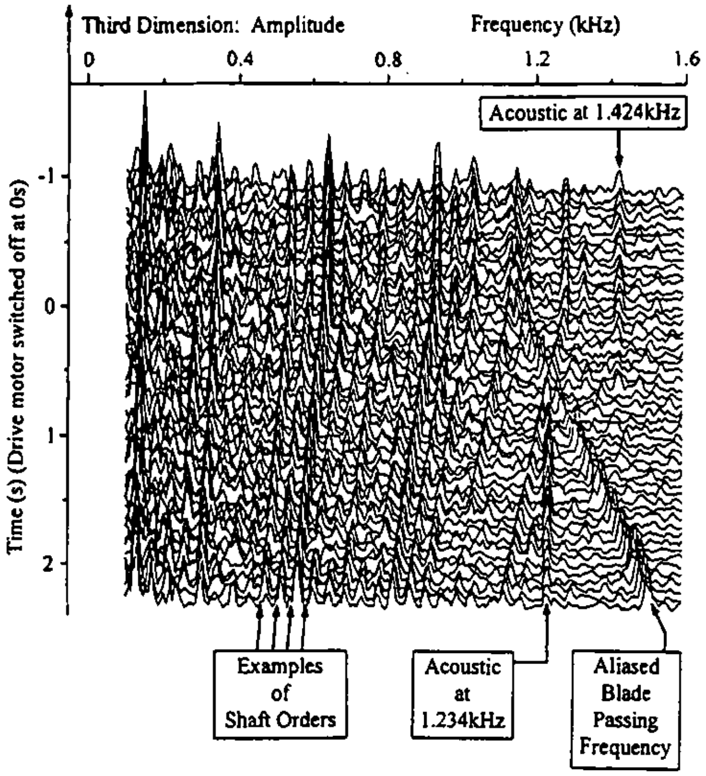

Figure 5. Pressure amplitude spectra as a function of deceleration time

$$M_\theta = \frac{2\pi r_{tip} f}{mc}$$

Taking $m = 1$, $f = 204$Hz, $r_{tip} = 254$mm, $c = 344$m/s (speed of sound at 295K), gives $M_\theta = 0.95$. We see that these modes are cut-off because the value of M_θ is less than unity at the tip radius (and therefore lower still at other radii). A more rigorous calculation of this Mach number (or 'cut-off ratio') can be performed for a particular mode at the respective propagation radius (at which a plane uniform wave appears to propagate at the velocity of sound). For a mode 7 pattern the propagation radius is 223.9mm and M_θ equals 0.83. This value is consistent with values that have been measured on high-speed compressors which have been found to lie between 0.8 and 0.9.

It is likely that the two remaining signals shown in Figure 4 at 1176Hz and 1570Hz are the 23rd and 31st harmonics of the shaft frequency (49.1Hz). Close examination of Figure 4 reveals that as the flow coefficient through the compressor was increased, the amplitudes

Table 1. Measured acoustic frequencies expressed as factors of 204Hz

Frequency (Hz)	Multiple of 204Hz
1022	5.01
1234	6.05
1424	6.98
1622	7.95

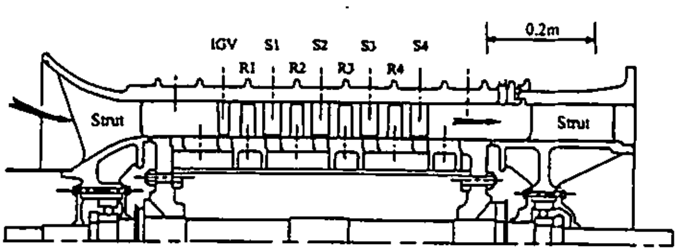

Figure 6. Cross-sectional view of the C106 compressor

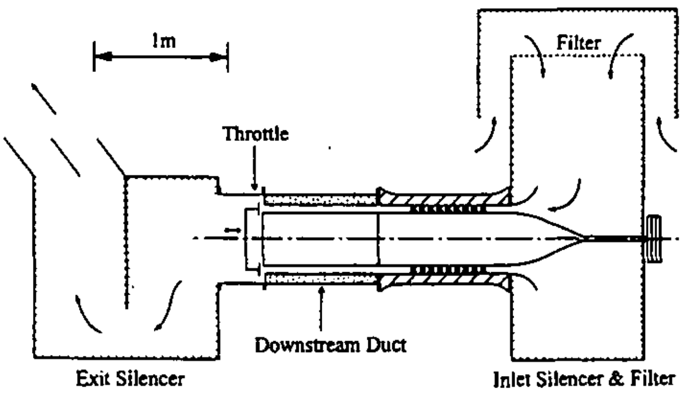

Figure 7. Schematic layout of the C106 facility

of the acoustic signals varied such that the largest amplitudes moved to higher frequency components. At a flow coefficient of 0.70 the largest amplitude of the acoustic signals occurs at 1022Hz. At a higher flow coefficient of 0.76 the largest amplitude acoustic signal occurs at 1234Hz, while at a still higher flow coefficient of 0.81 the largest amplitude acoustic signal occurs at 1424Hz. This stepping in frequency of the signal is a characteristic of acoustic resonance and is consistent with the hypothesis that vortex shedding is the excitation mechanism.

Changes in the Spectrum with Shaft Speed

A characteristic of acoustic resonance as observed in high-speed compressors is that the frequency associated with any particular wave structure is approximately independent of shaft speed. (The degree to which the frequency is exactly constant is a function of the damping of the acoustic signal, as found by Smith, 1991.) Although the C106 compressor does not have variable speed control, a series of spectra was measured using a Kulite transducer mounted at the IGV inlet plane while the power to the drive motor was switched off and the shaft allowed to decelerate. The results of these measurements are shown in Figure 5 as a carpet plot of pressure spectra. During the first two seconds of deceleration, the most prominent acoustic signal is the component at 1234Hz which remains at a constant frequency while the frequencies of the surrounding shaft orders fall. This characteristic of the C106 acoustic phenomenon is therefore consistent with experience of acoustic resonance in high-speed compressors. (The aliased component at blade passing frequency shown in this figure was present despite low-pass filtering the signal at 2kHz owing to the very large amplitude of this signal.)

Changes in the Spectrum with Duct Length

When studying an acoustic phenomenon, it is necessary to consider all volumes of the compression system. Figure 6 shows details of the compressor and the positions of six struts in the bearing housings at compressor inlet and exit, while Figure 7 shows the associated ducting upstream and downstream of the compressor. The frequency of an acoustic resonance signal, as described above, depends on the circumferential order of the wave, m, and on the effective speed of sound in the circumferential direction, $M_\theta c$. From equation 2,

$$\omega = \frac{m M_\theta c}{r_o} \qquad (7)$$

where M_θ depends principally on the solidity of the blading, as shown by Meyer and Neumann (1972). The frequencies of acoustic resonance signals are therefore not predicted to depend on the axial length of the compression system. To test the C106 acoustic phenomenon against this criterion, tests were performed using three different lengths of ducting between the compressor and the downstream throttle. The short, datum and long ducts produced distances of 1070mm, 1270mm and 1770mm between the stator 4 exit plane and the throttle valve respectively. In each case the exit ducting was annular with the same inner and outer radii as the compressor section. For each length of duct, the compressor geometry and flow coefficient were set to give the same operating point (as previously described) and pressure spectra were measured using a Kulite transducer mounted at the stator 4 exit plane.

Table 2. Comparison of acoustic frequencies measured at 3 duct lengths

Duct Length: S4 t.e.→throttle (mm)	Frequency at Peak Amplitude f_{pk} (Hz)	Ambient Temperature T_{amb} (K)	$f_{pk} \times \sqrt{\frac{288}{T_{amb}}}$
1067	1417.5	294.4	1402.1
1274	1418.9	295.0	1402.1
1771	1422.5	296.5	1402.1

The results of these measurements are summarised in Table 2 which shows the frequencies corresponding to the peak amplitude of the acoustic signal and the ambient temperatures at which the spectra were measured. After normalising these frequencies to account for variations in the speed of sound with temperature it was found that the acoustic frequency was exactly constant at 1402.1Hz for each of the three duct lengths. These results show that the frequency of the acoustic signal was independent of changes in the axial length of the compression system and that, in this respect, the structure of the wave is consistent with the theoretical description given earlier.

Phase Variation

The structure of the acoustic signal in the C106 was investigated using arrays of 8 Kulite transducers to measure changes in the phase and amplitude of the signal in the axial and circumferential directions in the compressor and downstream duct. The distributions of amplitude and phase were measured by calculating the cross-spectra of the signals from transducers 2-8 using transducer 1 to provide a datum signal. To calculate the spectra from each channel, 4096 samples were measured from each transducer with a sampling period of 170μs, thereby giving a resolution in the frequency domain of 0.7Hz. To improve the consistency of the results, 50 cross-spectra were calculated for each of transducers 2-8 during each sampling event. These were ensemble-averaged to give 7 cross-spectra (one for each of transducers 2-8) which were subsequently used to compare phase and amplitude. Prior to these measurements the gains and phase shifts introduced by the different transducers were measured and these were accounted for during the data processing to ensure valid comparisons of signal amplitude and phase.

Measurements were made for a large number of distributions of the 8 transducers in both the compressor and the downstream duct. The transducers were mainly distributed either axially or circumferentially, although a number of rectangular arrays were also used. Spectra were measured for each of the three lengths of downstream ducting, although only the results for the datum duct are presented here as the results for the longer and shorter ducts were found to be similar. The measurements were performed at the same compressor geometry and flow coefficient as previously described and the acoustic signal at approximately 1420Hz was therefore the main subject of the investigation. Small changes in this frequency were observed during the course of the experiments but these changes were found to be consistent with changes in the ambient temperature.

Phase Variation in the Compressor. Figure 8 shows the results of a circumferential measurement of phase in the compressor section at the stator 4 exit plane. These results are significant because they confirm that the structure of the 1420Hz signal has order 7 in the circumferential direction, as suggested by the preliminary results given in Table 1. The sign of the gradient of the phase distribution in Figure 8 indicates that the pressure field rotates in the opposite direction to rotor rotation (a 'backward' travelling wave). Both forward and backward travelling waves have been observed in high-speed compressors. The distribution of phase shown in Figure 8 is not an exactly straight line; however, when the measurements were repeated, an almost identical phase distribution was found, suggesting that the departure of the points from the straight line shown in the figure is not due to inadequate averaging. Instead, it indicates that there may be more than one acoustic mode present at this frequency, although the mode with circumferential order 7 is the most prominent. The confirmation of a mode of circumferential order 7 in the compressor also confirms the value of M_θ as 0.84 and that the structure of the wave in the compressor is cut-off.

Measurements of phase change with axial distance in the compressor section were found to be more difficult to interpret than the circumferential measurements, owing to the regular, wide spacing of the measurement planes in the compressor and the unknown effects of spatial aliasing. Figure 9 shows the results that were obtained when the 8 transducers were aligned axially, from the IGV exit plane (0mm), through the stator exit planes (91.5mm to 366mm) and continuing into the downstream bearing housing (457.5mm to 652.5mm). To identify trends in the data, it was found helpful to plot the measured phase values and points at $\pm 2\pi$ radians, as shown in the figure. Because of the possibility of spatial aliasing, lines A, B and C in Figure 9 (and

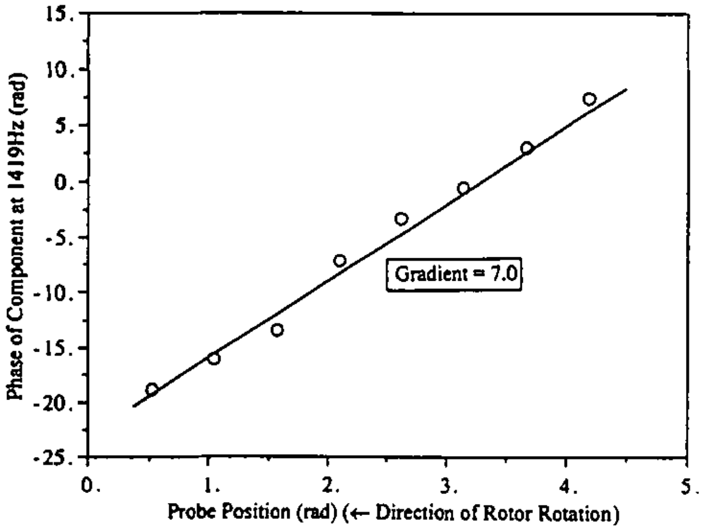

Figure 8. Circumferential phase distribution in the compressor

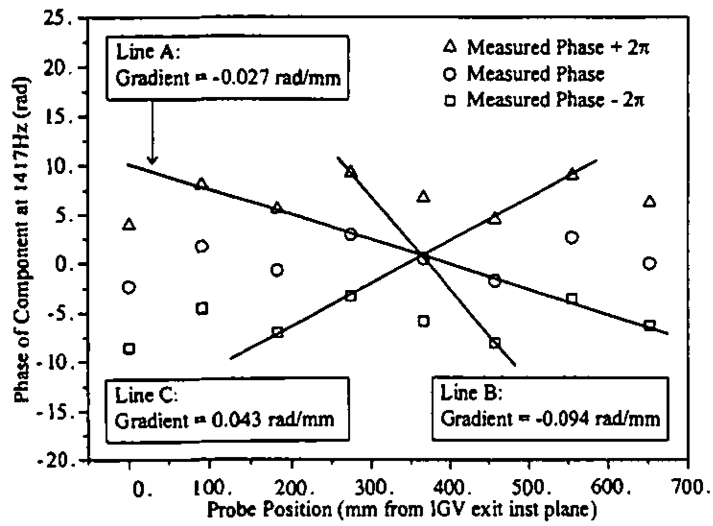

Figure 9. Axial phase distribution in the compressor

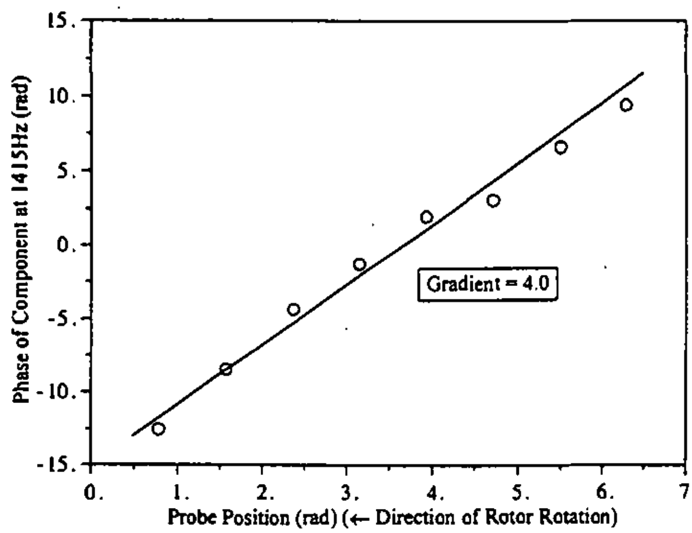

Figure 10. Circumferential phase distribution in the downstream duct

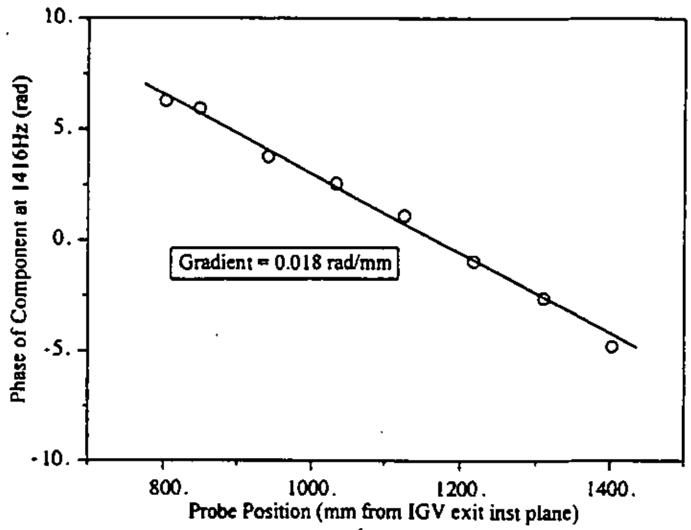

Figure 11. Axial phase distribution in the downstream duct

lines of progressively more positive and more negative gradient) are equally valid interpolations between the measured data points. To increase confidence in one of these possible solutions it would be necessary to repeat these measurements with a narrower or alternatively less regular spacing of the transducers. At the time of performing these experiments, transducer access was limited to regularly spaced instrumentation planes between the blade rows and so it was not possible to increase the spatial definition beyond that observed in Figure 9. The issue of spatial aliasing did not confuse the interpretation of circumferential phase measurements however, firstly because the circumferential order is constrained to be an integer value and secondly because the frequency measurements in Table 1 suggest that an order 7 mode existed, and therefore that the phase results did not describe a structure with a fundamental order of 14, 21 or 28 etc.

Phase Variation in the Duct. Circumferential and axial distributions of phase were measured in the downstream ducting in a similar manner to the phase measurements in the compressor. Measurements in the duct benefited from arrays of instrumentation holes which were more closely spaced than in the compressor section. In the case of axial measurements of phase, this reduced the uncertainty in the interpretation of the data introduced by the possibility of spatial aliasing. Despite the frequency of the acoustic signal being the same in the bladed region and downstream ducting, the structure of the acoustic wave was found to be very different in the two sections. In particular, the results of phase measurements in a circumferential direction, summarised in Figure 10, suggest that the wave has a circumferential order of 4 in the duct, as opposed to order 7 in the compressor. This difference is structure between the waves in the compressor and duct sections is somewhat surprising but is supported by the results of a number of separate circumferential phase

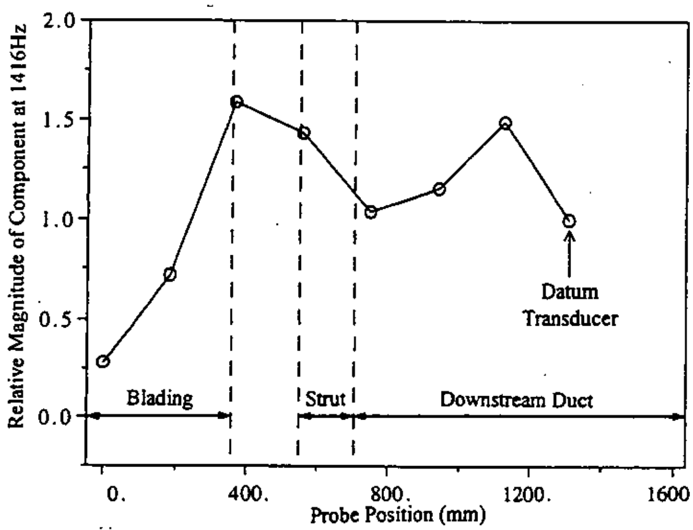

Figure 12. Axial distribution of the amplitude of acoustic signal at 1416Hz

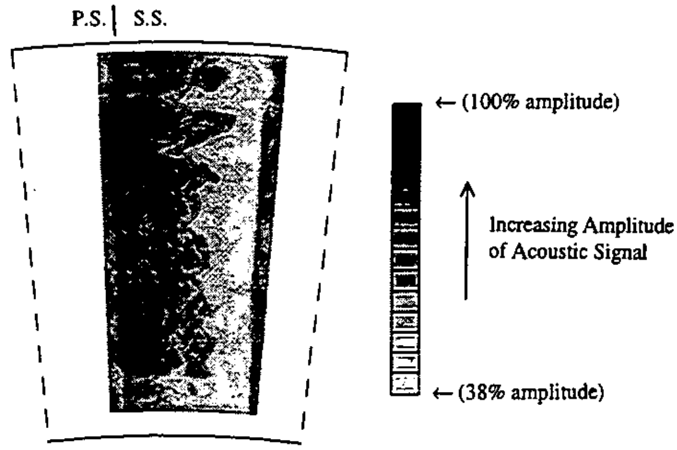

Figure 13. Amplitude distribution of the acoustic signal over the stator 4 exit plane

measurements in both sections. Once again, the small deviations of the data points from the straight line in Figure 10 were found to be repeatable, suggesting the presence of more than one mode at this frequency. The circumferential Mach number of this mode, calculated using equation 2, was found to be 1.45, showing that this wave is cut-on. At present it is not understood how these two modal structures interface at the boundary between the compressor and the duct. It may be that modes of order 4 and 7 are both generated by the acoustic phenomenon; the order 7 mode dominates in the compressor but, being cut-off, decays rapidly with axial distance in the duct, where the order 4 mode is dominant.

The measurements of phase in an axial direction in the duct are plotted in Figure 11, which shows that the phase of the signal changes at a rate of 0.018 radians per millimetre of duct length. The slopes of the lines shown in Figures 10 and 11 suggest that the wave in the duct has a helical structure and that it propagates downstream, rotating in a direction against rotor rotation. The direction of rotation is thus the same as the mode 7 wave detected in the bladed section.

Amplitude Variation

The axial variation of the acoustic amplitude was measured using 8 Kulite transducers positioned in various axial arrays through the compressor and downstream duct. The cross-spectrum method was used to measure the ensemble-averaged distribution of amplitude, relative to the amplitude measured by the first transducer.

The results of these amplitude measurements are summarised in Figure 12, which shows the measured amplitudes from a widely spaced array of transducers positioned over the blading, the rear struts and the downstream duct. This figure shows that the amplitude of the acoustic signal increases rapidly with axial distance through the compressor and reaches a maximum close to the stator 4 exit plane, as confirmed by more detailed measurements in this region. The amplitude reduces with distance through the rear bearing housing and strut and shows varying levels in the downstream duct. We might speculate that energy does not propagate beyond the throttle (and therefore that energy is trapped within the system) if the acoustic wave is reflected by the flat surface of the throttle plate, which is perpendicular to the compressor axis as shown in Figure 7.

To measure the amplitude of the acoustic signal over the stator exit flow-field, a total pressure probe containing a Kulite transducer was traversed in the stator 3 and stator 4 exit planes at the acoustic resonance condition. The probe used for these traverses was specially designed to have a high frequency-response. The probe was traversed over a grid of 37 radial by 25 circumferential points which covered one stator passage. At each point, the probe was rotated to face the direction of the time-averaged flow (previously measured by traversing a hot-wire probe) and the pressure signal was sampled. Twenty spectra were calculated at each point from measurements of the pressure signal, and these were ensemble-averaged to give a representative spectrum at each point. Although it is not clear that perturbations in total pressure can be classified as an *acoustic* signal, the spectra that were measured using the total pressure probe contained clear peaks at the previously determined acoustic frequencies. In Figure 13 the amplitudes of these components are shown contour plotted, using results of the traverse at the stator 4 exit plane. These results suggest that the amplitude of the acoustic signal is greatest on the suction side of the stator wake and that it gradually decreases toward the pressure side of the adjacent blade. The amplitude of the signal changes rapidly over the stator wake but varies very little in the spanwise direction. A similar result was found at the stator 3 exit plane. These results are the first measurements of the amplitude of an acoustic resonance signal to be made inside a compressor flow-field. They confirm recent theoretical work by Parker (1995) which suggests that the amplitude of an acoustic signal varies in the pitchwise direction.

Strouhal Numbers

Finally, we consider the Strouhal numbers of the support struts and the rotor and stator blades at the experimental operating point to find possible sources of vortex shedding in the compressor. As noted earlier it cannot be assumed that Strouhal numbers are exactly equal to 0.2 at a resonant condition; however this value provides a useful guide in the absence of detailed measurements of the flow-field in the blade trailing edge regions.

The six struts in each of the upstream and downstream bearing housings are aligned axially and have a trailing edge thickness of 8mm. For a vortex shedding frequency of 1420Hz at a flow coefficient of 0.85, these struts have a Strouhal number based on trailing edge thickness of 0.195. This value is clearly very close to the value of 0.20 at which isolated flat plates are observed to shed vortices, suggesting that the struts are possible sources of vortex shedding. Conflicting evidence is given, however, by the axial distribution of amplitude (Figure 12) which shows that the acoustic signal is weak in the region of the upstream struts and that the amplitude is decaying in the region of the downstream struts.

Because the rotor and stator blades are subject to large values of incidence, the calculation of the Strouhal numbers of these blades is complicated by the requirement that the length scale used to define the Strouhal number should represent the width of the wake and not simply the trailing edge thickness. As Figure 3 shows, the width of the stator 3 wake at the experimental operating point is considerably wider than the thickness of the trailing edge. If D represents the trailing edge dimension which gives a Strouhal number, based on this dimension, of 0.2, then D/Ch can be calculated as the ratio of the Strouhal number based on D, to the Strouhal number based on chord,

$$\frac{D}{Ch} = \frac{fD/_V}{fCh/_V} = \frac{0.2}{St_{chord}} \qquad (8)$$

The dimension D can also be expressed as a proportion of the blade spacing s by dividing D/Ch by the space-chord ratio. In Table 3 below, the values of St_{chord}, D/Ch and D/s are tabulated for the inlet guide vane, rotor and stator rows, assuming that each sheds vortices corresponding to the measured signal at 1420Hz at a flow coefficient of 0.85. The Doppler shift in frequency experienced by the rotor was accounted for in these calculations.

Table 3. Strouhal number results

Blade Row	St_{chord}	D/Ch	D/s
IGV	0.86	0.23	0.36
Rotor	0.79	0.25	0.37
Stator	0.86	0.23	0.36

Although it has not been proved that vortex shedding is the excitation mechanism that drives acoustic resonance in high-speed compressors, general experience of gas turbine manufacturers suggests that Strouhal numbers based on chord for blade rows which are exciting acoustic resonance are approximately 0.6 if vortex shedding is present. Table 3 shows that the Strouhal numbers of all blade rows in the C106 exceed this value although the values of D/s (the wake dimension as a proportion of blade spacing) look plausible for each row. In particular, the value of D/s for the stator is close to a value that one might estimate from Figure 3. From this study of Strouhal numbers we conclude that the struts and blade rows in the compressor are all possible sources of vortex shedding. More detailed measurements of the flow in the vicinity of the trailing edges would be necessary to determine with certainty which blade rows, if any, are exciting acoustic resonance by a vortex shedding mechanism.

CONCLUSIONS

The results of the experiments on the C106 compressor presented in this paper comprise the first systematic measurements of a resonant acoustic phenomenon on a low-speed multistage compressor. The experiments revealed that the C106 phenomenon shares many characteristics with acoustic resonances measured in high-speed compressors. These include:

1) A lobed pressure pattern which rotates around the annulus with a circumferential Mach number of 0.83 (values measured on high-speed compressors have been found to lie between 0.8 and 0.9).

2) Several acoustic frequencies at equal intervals, corresponding to different circumferential orders of the rotating pressure field.

3) Step changes in frequency as modes change to higher circumferential order as the flow coefficient through the compressor is increased.

4) An acoustic frequency (of the most studied mode) which is approximately independent of flow coefficient, shaft speed and axial length of the downstream duct.

6) Additionally, the first measurements of an acoustic signal within the blade-to-blade flow-field showed that at the stator exit planes the amplitude of the signal varies considerably in the pitchwise direction but that it changes very little across the span.

ACKNOWLEDGEMENTS

The author would like to thank Rolls-Royce plc for supporting the research described in this paper and for allowing publication of the results.

REFERENCES

Camp, T. R., 1995, "Aspects of the Off-Design Performance of Axial Flow Compressors," Ph.D. Dissertation, Cambridge University Engineering Department.

Cargill, A. M., 1993, Private Communication, March 31.

Cumpsty, N. A., and Whitehead, D. S., 1971, "The Excitation of Acoustic Resonance by Wake Shedding," Journal of Sound and Vibration, Vol.18, No.3., pp.353-369.

Koch, W., 1985, "Local Instability Characterisitics and Frequency Determination of Self-Excited Wake Flows," Journal of Sound and Vibration, Vol.99, No.1, pp.53-83.

Meyer, E., and Neumann, E. G., 1972, "Physical and Applied Acoustics," New York Academic Press, pp.191-192.

Parker, R., 1967, "Resonance Effects in Wake Shedding from Compressor Blading," Journal of Sound and Vibration, Vol.6, No.3, pp.302-309.

Parker, R., 1968, "An Investigation of Acoustic Resonance Effects in an Axial Flow Compressor Stage," Journal of Sound and Vibration, Vol.8, No.2, pp.281-297.

Parker, R., and Stoneman, S. A. T., 1985, "An Experimental Investigation of the Generation and Consequences of Acoustic Waves in an Axial Flow Compressor: Large Axial Spacings Between Blade Rows," Journal of Sound and Vibration, Vol.99, No.2, pp.169-182.

Parker, R., and Stoneman, S. A. T., 1989, "The Excitation and Consequences of Acoustic Resonances in Enclosed Fluid Flow around

Solid Bodies," Proc. I.Mech.E., Vol.203, pp.9-19.

Parker, R., 1995, Private Communication, January 22.

Smith, N. H. S., 1991, "Investigation into the Supression of Acoustic Resonances," Ph.D. Dissertation, University College of Swansea.

Tyler, J. M., and Sofrin, T. G., 1962, "Axial Flow Compressor Noise Studies," Trans. Society of Automotive Engineers, Vol.70., pp.309-332.

Welsh, M. C., and Gibson, D. C., 1979, "Interaction of Induced Sound With Flow Past a Square Leading Edged Plate in a Duct," Journal of Sound and Vibration, Vol.67, No.4, pp.501-511.